



# Spatial variance in the 12-lead ECG and mechanical dyssynchrony

María Paula Bonomini<sup>1</sup> · Hugo Villarroel-Abrego<sup>2</sup> · Raúl Garillo<sup>3</sup>

Received: 17 February 2021 / Accepted: 15 April 2021  
© Springer Science+Business Media, LLC, part of Springer Nature 2021

## Abstract

**Introduction** Electrical transmission disorders have a deleterious effect on cardiac depolarization, resulting in a disorganized ventricular contraction that reduces global mechanical efficiency; this mechanical dyssynchrony can be corrected by cardiac resynchronization therapy. However, despite adjustments in the electrical criteria selection of QRS for the recognition of mechanical dyssynchrony, a significant proportion of patients do not currently respond to this therapy.

**Purpose** To find if a new predictor of dyssynchrony, the electrocardiogram spatial variance, is a better marker of mechanical dyssynchrony than QRS duration.

**Methods** Forty-seven electrocardiograms and 47 strain (2D speckle tracking) echocardiograms were prospectively collected simultaneously in consecutive, non-selected patients; the left ventricular mechanical dispersion was measured in all the cases. The electrocardiographic analysis of variance was made with a digital superposition of the electrocardiographic leads and generates different indexes of variance of both QRS complex and repolarization phase.

**Results** ROC analysis probed that the best area under the curve (AUC) value correlated with left ventricular mechanical dispersion and was obtained combining several spatial variance markers (considering depolarization and repolarization spatial variance together; AUC = 0.97); the same analysis using the QRS duration versus mechanical dispersion showed a significantly lower AUC value (AUC = 0.64).

**Conclusion** Spatial variance combining depolarization and repolarization markers is a superior predictor of left ventricular mechanical dispersion than QRS duration.

**Keywords** Mechanical dyssynchrony · 2D speckle tracking · Spatial variance

## 1 Introduction

In recent years, cardiac electrical dyssynchrony has increasingly gained attention as an endpoint in cardiac resynchronization therapy (CRT). A growing body of evidence supports that intraventricular dyssynchrony, not always related with QRS duration, is the main cause for CRT application [1, 2], and therefore, many studies have recently attempted to infer

other cardiac dyssynchrony markers from the 12-lead ECG. Approaches has focused on temporal features, mainly covering differences in intrinsicoid deflections [3], standard deviations of activation times in body surface isochronal maps [4], or index from ultrahigh frequency ECG techniques [5].

Spatial variance (SV) of the 12-lead ECG represents the degree of electrical heterogeneity in the heart. When aberrant electrical circuits are generated in the specialized conduction circuit, the ECG lead morphologies get distorted. In this condition, electrical heterogeneity increases. Recently, some research groups reported electrical dyssynchrony markers based on ventricular depolarization dispersion, measured as the depolarization spatial variance [6] or based on correlation analysis [7, 8]. Although these are promising approaches, these markers never reported a relationship to a gold standard measurement such as left ventricular mechanical dyssynchrony (MD), measured by 2D speckle tracking strain echocardiography (STE). Villarroel and Garillo [9] recently published a paper about the accuracy of a very

✉ María Paula Bonomini  
paula.bonomini@conicet.gov.ar

<sup>1</sup> Instituto Argentino de Matemática (IAM), CONICET, Instituto de Investigaciones Biomédicas (IIBM), University of Buenos Aires (UBA), Buenos Aires, Argentina

<sup>2</sup> Hospital de Diagnóstico Escalón, Facultad de Medicina, Universidad Salvadoreña Alberto Masferrer, San Salvador, El Salvador

<sup>3</sup> Facultad de Ciencias Médicas, Pontificia Universidad Católica Argentina, Buenos Aires, Argentina

simple variance index of the QRS of just 2 ECG leads, DII and V6, using the SynchroMax™ device, to predict or rule out MD, in comparison with QRS mean duration, in a cohort of 54 patients STE, excluding patients with transmural myocardial infarction; they concluded that this simple repolarization variance index had better sensitivity and negative predictive value respect to the average QRS duration alone, for the diagnosis of left ventricular MD.

The analysis of cardiac electrical dyssynchrony has been always limited to the depolarization phase. However, with the appearance of aberrant electrical paths and the consequent distortion of the depolarization front, it is natural to expect secondary alterations in repolarization. Our objective was to extend the analysis of spatial variance to both cardiac phases, depolarization and repolarization, measuring the ability of each marker to explain the MD measured by STE.

## 2 Materials and methods

Patients who had an appointment for an STE between the months of August 2018 and July 2019 were studied at the Cardiovascular Center of Hospital de Diagnóstico Escalón, San Salvador, El Salvador.

### 2.1 Inclusion criteria

- Patients older than 18 years.
- Subjects whose longitudinal subendocardial strain images by speckle tracking were technically satisfactory in at least 14 of 16 the segments into which the left ventricular myocardium is traditionally divided.

The STE studies were performed with Acuson SC2000 equipment (Siemens Healthcare GmbH), with 2D speckle tracking technique. The standard deviation of time for maximum longitudinal subendocardial deformation of all left ventricular segments, the so-called mechanical dispersion (normal value less than 56 ms, severe dyssynchrony greater than 70 ms), was calculated. Once the STE was completed, having confirmed that the patient met the criteria detailed above, with prior informed consent, a standard 12-lead electrocardiogram (ECG) was performed, with speed of 25 mm/s and voltage 10 mm/1 mV, using SynchroMax™ (EXO, Buenos Aires, Argentina). The average QRS duration of the 12 standard leads was calculated. The cut-off value for diagnosing abnormal left ventricular mechanical dispersion was set at 56 ms.

### 2.2 Study population

The group studied included 45 patients of both sexes, 25 men (55.6%) and 20 women (44.4%), of whom 47

electrocardiographic traces and 47 echocardiograms were obtained with evaluation of left ventricular MD by STE. The average age was 66.2 + 14.8 years. Table 1 summarizes the cardiac pathologies of the patients. Six of them had implanted electronic devices (13.3%: two resynchronizers, two single-chamber pacemakers with right ventricular pacing, one AAI-programmed left atrial unicomeral pacemaker, and one dual-chamber pacemaker with DDD pacing).

### 2.3 Electrical dyssynchrony

Three different markers of electrical dyssynchrony were compared: spatial variance (SV), which measures morphological dispersion between groups of similar leads; correlation analysis, which measures similarity between pairs of leads; and the duration of the QRS complex.

#### 2.3.1 Spatial variance (SV)

SV quantifies the maximum Euclidean distance of every lead within an ensemble from the lead ensemble average. Therefore, SV can assign a numeric value to the different morphological ECG patterns involving two or more leads. In normal conduction patients, some inter-lead sets can produce high SV values while others can produce low SV

**Table 1** Cardiac conditions in the 47 patients recruited for this study

	<i>n</i>	%
Cardiac condition		
Dyssynchrony index (SynchroMax) > 0.4	29	61.7
Abnormal mechanical dispersion	22	46.8
QRS < 120 ms	29	61.7
Non-sinus rhythm	5	10.6
Pacemaker rhythm	5	10.6
Sick sinus syndrome	1	2.1
Structural heart disease		
Heart failure	20	42.5
Myocardial infarction	8	17.0
Hypertensive left ventricular hypertrophy	6	12.8
Hypertrophic cardiomyopathy	1	2.1
Non-compaction cardiomyopathy	1	2.1
Takotsubo cardiomyopathy	1	2.1
Mitral valve prolapse	1	2.1
Conduction abnormalities		
Advanced left bundle branch block	7	14.9
Bifascicular block	4	8.5
Right bundle branch block	3	6.4
Left anterior fascicular block	2	4.2
Left posterior fascicular block	1	2.1
Nonspecific intraventricular conduction block	1	2.1
Bayés syndrome	1	2.1

values, depending on their similarity in morphology. Thus, two extreme scenarios for maximum ( $SV^{QRS_{max}}$ ) and minimum ( $SV^{QRS_{min}}$ ) SV in normal subjects were proposed. In [9], there is a detailed description of the method. In this piece of work, a particular set of 3 leads was proposed for either the maximal (aVR-V1-V6) or minimal (II-aVF-V5) scenarios of SV. The SV was computed for the mentioned leads on an 80-ms window centered on the QRS complex. To reduce parameters, the maximum and minimum SV values were combined into a ratio. The ratio between maximum and minimum variance was denoted as  $SV^{QRS_r}$ . The repolarization counterparts were denoted consistently as  $SV^{T_{max}}$ ,  $SV^{T_{min}}$ , and  $SV^{T_r}$ . Repolarization SV values were computed on the same set of leads as for depolarization. This time, variance was computed on a 200-ms window starting 50 ms apart from the QRS peak in order to span most of the T wave morphology.

### 2.3.2 Correlation analysis

Correlation analysis between leads also contributes to spatial heterogeneity, restricted to pairs of leads. In this way, the cross-correlation between leads II and V6, for example, can be informative about conduction alterations that occur mainly in the lower and left sides of the heart, such as left bundle branch blocks or left anterior hemiblock. In preserved conduction patients, the intrinsic deflections of both leads are conserved, and then the correlation signal will be centered at zero millisecond. On the contrary, if electrical ventricular conduction is not preserved, the maximum signal of the cross-correlation between the pair of leads will be

broadened and with a latency (maximum at nonzero lag, in millisecond). The original correlation mark was presented on leads II and V6 [7, 8]. From the original publication, only two parameters were analyzed, the shift of the peak of the cross-correlation signal ( $Corr_s$ , in ms) and the width of the cross-correlation signal ( $Corr_w$ , in ms) as measured at  $0.7 \times$  peak amplitude.

### 2.4 Statistical analysis

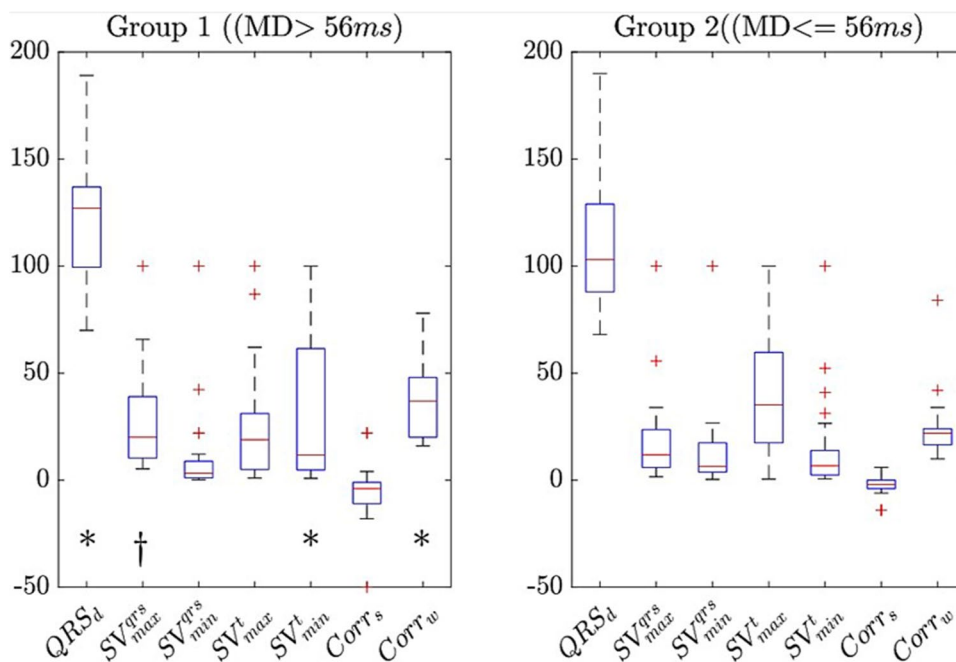
Continuous variables are presented as mean (SD) and compared by a nonparametric test, the unpaired two-sample Wilcoxon test. Significance level was set to 0.05. Categorical variables are presented as  $n$  (%) and compared using the  $\chi^2$  test and confidence intervals were calculated according to the recommended method given by Altman et al. [8].

Logistic regression analysis was used to investigate the relationship between electrical dyssynchrony markers and mechanical dyssynchrony. To avoid overfitting, a fivefold cross validation scheme was used. Since the number of cases ( $n=47$ ) was moderately low, no interaction terms were included in the models. Statistical calculations were performed using the Statistical Package for the Octave software.

## 3 Results

Table 1 shows the cardiac pathologies of the recruited patients. Figure 1 shows the distributions for the electrical dyssynchrony parameters analyzed in this study for

**Fig. 1** Boxplots for the mechanical dyssynchrony (DM) and the electrical dyssynchrony markers analyzed. QRS<sub>dur</sub>, QRS duration; SV<sub>qrs max</sub>, maximal depolarization spatial variance; SV<sub>qrs min</sub>, minimal depolarization spatial variance; SV<sub>T max</sub>, maximal repolarization spatial variance; SV<sub>T min</sub>, minimal repolarization spatial variance; Corr<sub>S</sub>, shift in the aVF-V<sub>5</sub> cross-correlation shift; Corr<sub>w</sub>, width in the aVF-V<sub>5</sub> cross-correlation width at  $0.7 \times$  Peak amplitude. \* $p < 0.05$ , † $p < 0.005$  against group 2, Wilcoxon test



dyssynchronous (group 1,  $n=20$ ) and non-dyssynchronous patients (group 2,  $n=25$ ). Notice that in the dyssynchronous cases, the depolarization variance for the set of leads aVR-V1-V6, the set with the most heterogeneous morphologies, decreased its dispersion ( $SV^{QRS}_{max}$ ; 27 vs 11  $mV^2$ ,  $p=5.9e-4$ ), while the set of minimal variance II-aVF-V5 increased the dispersion, even though it failed to meet statistical significance.

On the contrary, the repolarization variance decreased its maximum dispersion and significantly increased its minimum dispersion (26 vs 31  $mV^2$ ,  $p=0.0013$ ) in the dyssynchronous cases. This means that in the presence of conduction abnormalities, morphological variance goes further in the depolarization phase, growing even more in the maximum scenario and shrinking further in the minimum scenario. Exactly the opposite occurs with the repolarization phase. This means the maximum SV gets lower and the minimum SV gets higher in the presence of dyssynchrony.

The correlation analysis presented broader peak shifts in the II-V6 QRS peaks at group 1, with a significant widening (Corr<sub>w</sub>; 37 vs 24 ms,  $p=0.006$ ). This widening is a product of the QRS widenings in the actual leads II-V6.

Based on the aforementioned parameters, different logistic regression models were constructed to explain the MD measured by speckle tracking. Table 2 details separated models for the depolarization and repolarization spatial variance, the correlation analysis, and the traditional

**Table 2** Statistical performance for the different MD models based on electrical dyssynchrony parameters: Repolarization Variance, Depolarization Variance, Correlation analysis and QRSd. Notice the out-performance of the Repolarization model, producing the most significant of all of them

	Estimate	SE	t stat	<i>p</i>
Depolarization spatial variance				
Intercept	0.30947	0.33165	0.93311	0.35076
$SV^{QRS}_r$	1.8187	0.66964	2.7159	0.0066099
Chi <sup>2</sup> -statistics vs. constant model: 13, <i>p</i> -value = 0.00319				
Repolarization spatial variance				
Intercept	-0.52696	0.39783	-1.3246	0.18532
$SV^T_r$	-2.9966	0.97561	-3.0715	0.0021296
Chi <sup>2</sup> -statistics vs. constant model: 17.1, <i>p</i> -value = 3.52e-05				
Correlation analysis				
(Intercept)	-0.084067	0.30457	-0.27602	0.78254
Corr <sub>s</sub>	0.1635	0.28939	0.56497	0.57209
Corr <sub>w</sub>	-1.3001	0.44001	-2.9548	0.0031287
Chi <sup>2</sup> -statistics vs. constant model: 14.2, <i>p</i> -value = 0.000819				
QRS duration				
Intercept	0.028235	0.27075	0.10428	0.91694
QRS <sub>d</sub>	-0.57911	0.28572	-2.0269	0.042677
Chi <sup>2</sup> -statistics vs. constant model: 4.47, <i>p</i> -value = 0.0345				

QRS duration criteria. Surprisingly, the most significant model for MD based on electrical dyssynchrony parameters was the repolarization spatial variance ( $p=3.52e-5$ ), followed by the depolarization spatial variance ( $3.19e-4$ ) and correlation analysis ( $p=8.19e-4$ ). The QRSd model had the worst statistical significance ( $p=0.0345$ ). ROC analysis for the former models is displayed in Fig. 3. Note that the best area under the curve (AUC) values were obtained for the combined SV markers, depolarization and repolarization SV index, accounting in turn for both the maxima and minima scenarios in the following ratios:  $SV^{QRS}_r = SV^{QRS}_{min}/SV^{QRS}_{max}$  and  $SV^T_r = SV^T_{min}/SV^T_{max}$ . From now on, the combined  $SV^{QRS}_r$  and  $SV^T_r$  marker will simply be denoted as “SV.”

The improvement in the combined SV marker (AUC = 0.97) with respect to the correlation analysis (AUC = 0.78) and QRS duration (AUC = 0.64) was also transferred to the classification performances of the combined SV markers, with an accuracy of 89.8% as depicted in Fig. 2. Here, the confusion matrix for the combined SV marker is presented for a binary class (0: MD > 56 ms (group 1), 1: MD ≤ 56 ms (group 2)).

Finally, Figs. 3 and 4 illustrate the spatial variance curves for the set of leads aVR-V1-V6 and II-aVF-V5 for both the depolarization and repolarization phases (middle and lower panels) together with the correlation analysis for leads II-V6 (top panels) for a dyssynchronous representative patient and one with intact conduction, respectively. Notice the widening of the cross-correlation signal of the dyssynchronous case (Fig. 3) with respect to preserved conduction case (Fig. 4). Also, note the displacement of the cross-correlation peak from zero lag (0 ms) because of the shifts in the II-V6 QRS peaks in the dyssynchronous case, while the native conduction case presents a cross-correlation signal centered around 0 ms. Regarding the spatial variance, the shifts in either multi-lead set (aVR-V1-V6 or II-aVF-V5) in the dyssynchronous case produce an increased spatial variance.

## 4 Discussion

A quarter of a century ago, Cazeau et al. published a clinical case of refractory heart failure associated with prolonged QRS and mechanical dyssynchrony, treated with multichambered stimulation, laying the foundations for what was later called CRT [10]. Throughout these 25 years, several criteria employing the 12-lead ECG were used to identify subjects whose QRS alterations suggested the presence of MD, condition that could be corrected by CRT. Despite the adjustment in successive guidelines over time, a significant proportion of patients do not currently respond to this therapy.

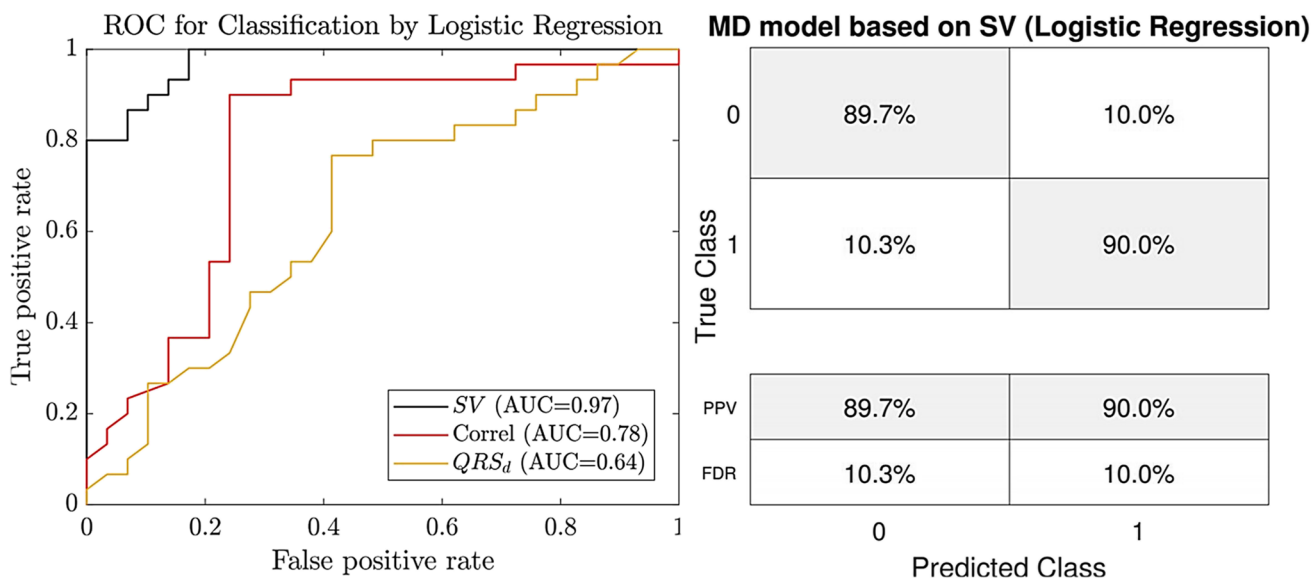


**Fig. 2** Performance for the MD model based on electrical dyssynchrony analysis. Left: ROC analysis for SV, Correl and QRSd markers. Right: confusion matrix for the SV model accounting for depolarization and repolarization spatial variance

Many studies aimed at quantifying depolarization dispersion. Turrini et al. [11] reported QRS dispersion as a

marker of cardiac risk in right ventricular cardiomyopathy. However, this method relied on temporal dispersion, the

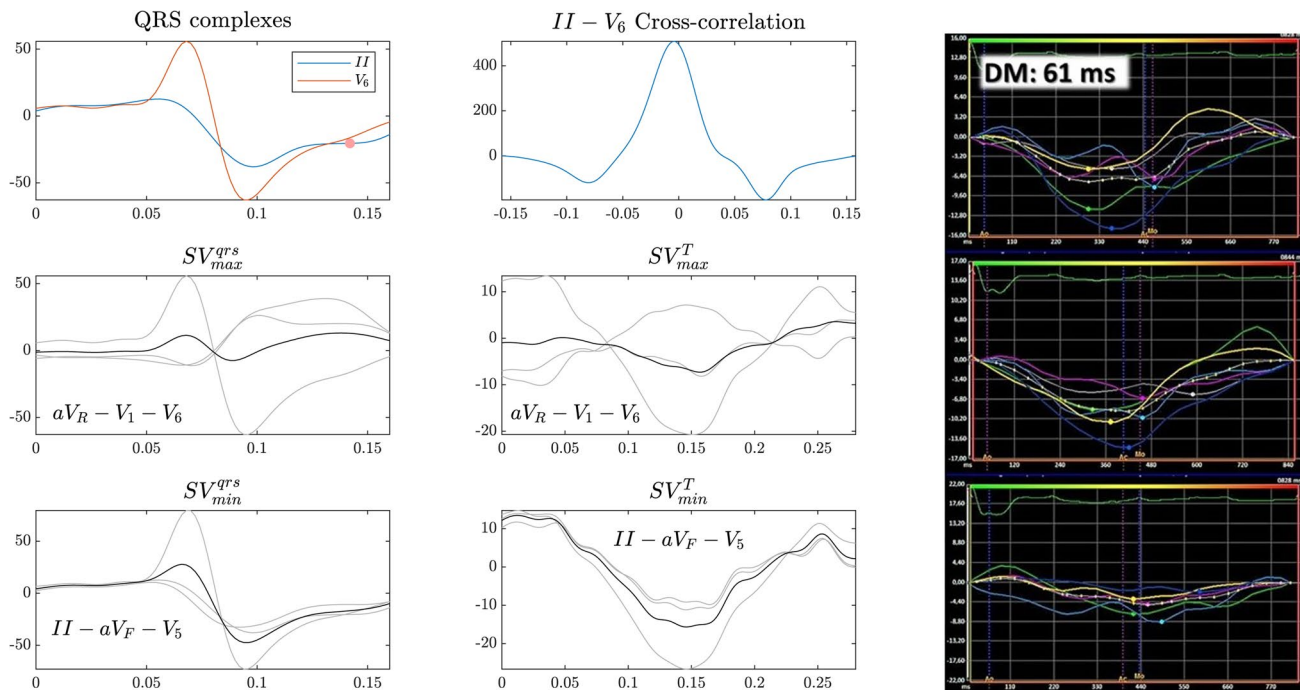


**Fig. 3** A case of electrical and mechanical dyssynchrony, with a pathological MD (61 ms). Representative analysis of correlation (top), maximal spatial variance (middle), and minima spatial variance (bottom). Notice the widened cross-correlation signal and the high T wave variance in the minima scenario and the high QRS variance

in the maxima scenario. Lead variances were computed about the mean morphology (black line). The right panel shows longitudinal strain curves of 4 chambers, 2 chambers, and 3 chambers apical views (STE)

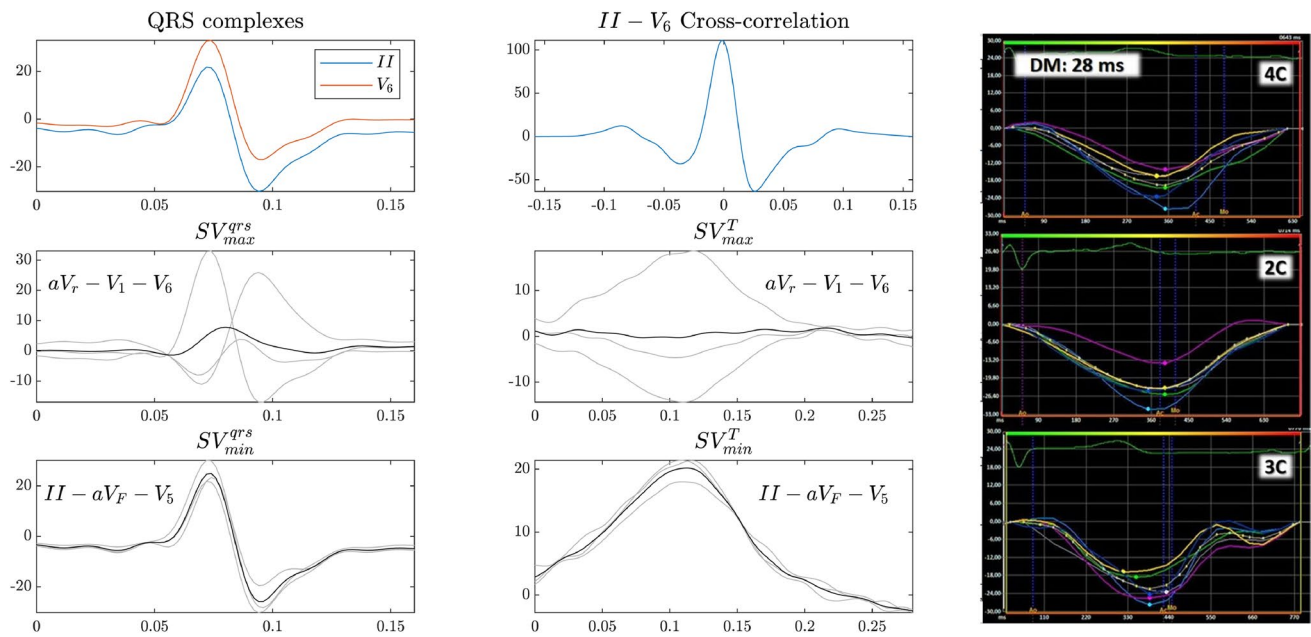


**Fig. 4** A case of preserved mechanical synchrony, with a normal MD (28 ms). Representative analysis of correlation (top), maximal spatial variance (middle), and minimal spatial variance (bottom). Lead vari-

ances were computed about the mean morphology (black line). The right panel shows longitudinal strain curves of 4 chambers, 2 chambers, and 3 chambers apical views (STE)

QT interval dispersion. Gage et al. quantified depolarization dispersion by measuring the standard deviation of activation times (SDAT) on a 53-electrode body surface isochronal map [4].

The SV makes use of the spatially distributed information contained in the 12-lead ECG. Nearing et al. applied SV to the QRS complex and to T waves, to predict cardiac risk in a set of heart failure patients [12]. The first attempt to associate SV to electrical dyssynchrony was reported by Bonomini et al. [13], where the depolarization variance outperformed the QRS duration at explaining the left ventricular electrical activation (LVED) measured by electrophysiology study in a set of dyssynchronous patients. The correlation analysis also achieved good correlation to the LVED in its original works [7, 8]. However, both studies lacked the inclusion of mechanical dyssynchrony information.

In the present paper the prediction of MD by assessing the duration of the QRS complex, the spatial variance of QRS and the combined spatial variance of QRS and T wave were compared against a reliable marker of dyssynchrony: MD measured with STE strain. The greatest predictive value was obtained with SV of the QRS depolarization combined with the T wave (repolarization) SV, offering a powerful tool to detect the presence of MD by measuring electrical dispersion.

## 5 Conclusions

Analysis of SV on the 12-lead ECG, especially when dispersion during depolarization (QRS complex) and repolarization (T wave) are analyzed together, turned out to be a valuable predictor of MD, a condition that can be corrected by cardiac resynchronization therapy.

**Data availability** Data can be available by request at any time.

## Declarations

**Ethical approval** The protocol was approved by the Ethics Committee of Hospital de Diagnóstico Escalón, San Salvador, El Salvador.

**Conflicts of interest** The authors declare no competing interests.

## References

1. Marek J, Saba S, Onishi T, Ryo K, Schwartzman D, Adelstein A, Gorcsan J. Usefulness of echocardiographically guided left ventricular lead placement for cardiac resynchronization therapy in patients with intermediate QRS width and non-left bundle branch block morphology. *Am J Cardiol.* 2014;113:107–16.
2. Hara H, Oyenuga O, Tanaka H, Adelstein E, Onishi T, McNamara D, Gorcsan J. The relationship of QRS morphology and mechanical dyssynchrony to long-term outcome following cardiac resynchronization therapy. *Eur Heart J.* 2012;33:2680–91.

3. Vereckei A, Szelenyi Z, Kutiyifa V, Szenasi ZG, Kiss M, Katona G et al. Novel electrocardiographic dyssynchrony criteria improve patient selection for cardiac resynchronization therapy. *EP Europace*. 2018;20(1):97–103.
4. Gage R, Curtin A, Burns K, Ghosh S, Gillberg J, Bank A. Changes in electrical dyssynchrony by body surface mapping predict left ventricular remodeling in patients with cardiac resynchronization therapy. *Heart Rhythm*. 2017;14:392–9.
5. Jurak P, Halamek J, Meluzin J, Plesinger F, Postranecka T, Lipoldova J, Novak M, Vondra V, Viscor I, Soukup L, Klimes P, Vesely P, Sumbera J, Zeman K, Asirvatham RS, Tri J, Asirvatham SJ, Leinveber P. Ventricular dyssynchrony assessment using ultra-high frequency ECG technique. *J Intervent Cardiac Electrophysiol*. 2017;49(3):245–54.
6. Bonomini M, Ortega D, Barja L, Logarzo E, Mangani N, Paolucci A. ECG parameters to predict left ventricular electrical delay. *J Electrocardiol*. 2018;51:844–50.
7. Ortega D, Logarzo E, Barja L, Paolucci A, Mangani N, Mazzetti E, Bonomini MP. Novel implant technique for septal pacing A noninvasive approach to nonselective his bundle pacing. *J Electrocardiol*. 2020;63:35–40.
8. Bonomini MP, Ortega DF, Barja LD, Mangani NA, Paolucci A, Logarzo E. Electrical approach to improve left ventricular activation during right ventricle stimulation. *Medicina (Buenos Aires)*. 2017;77:7–12.
9. Villarroel-Ábrego H, Garillo R. Índice de varianza versus duración del complejo QRS para el diagnóstico de dispersión mecánica del ventrículo izquierdo. *Insuf Card*. 2020;15(1):2–9.
10. Cazeau S, Ritter P, Bakdach S, Lazarus A, Limousin M, Henao L, Mundler O, Daubert JC, Mugica J. Four chamber pacing in dilated cardiomyopathy. *Pacing Clin Electrophysiol*. 1994;17(1 Pt 2):1974–9.
11. Turrini P, Corrado D, Basso C, Nava A, Bauce B, Thiene G. Dispersion of ventricular depolarization–repolarization. *Circulation*. 2001;103(25):3075–80.
12. Nearing BD, Wellenius GA, Mittleman MA, Josephson ME, Burger AJ, Verrier RL. Crescendo in depolarization and repolarization heterogeneity heralds development of ventricular tachycardia in hospitalized patients with decompensated heart failure. *Circ Arrhythm Electrophysiol*. 2012;5(1):84–90.
13. Bonomini MP, Ortega DF, Barja LD, Mangani N, Arini PD. Depolarization spatial variance as a cardiac dyssynchrony descriptor. *Biomed Signal Process Control*. 2019;49:540–5.

**Publisher's note** Springer Nature remains neutral with regard to jurisdictional claims in published maps and institutional affiliations.

## Terms and Conditions

Springer Nature journal content, brought to you courtesy of Springer Nature Customer Service Center GmbH (“Springer Nature”).

Springer Nature supports a reasonable amount of sharing of research papers by authors, subscribers and authorised users (“Users”), for small-scale personal, non-commercial use provided that all copyright, trade and service marks and other proprietary notices are maintained. By accessing, sharing, receiving or otherwise using the Springer Nature journal content you agree to these terms of use (“Terms”). For these purposes, Springer Nature considers academic use (by researchers and students) to be non-commercial.

These Terms are supplementary and will apply in addition to any applicable website terms and conditions, a relevant site licence or a personal subscription. These Terms will prevail over any conflict or ambiguity with regards to the relevant terms, a site licence or a personal subscription (to the extent of the conflict or ambiguity only). For Creative Commons-licensed articles, the terms of the Creative Commons license used will apply.

We collect and use personal data to provide access to the Springer Nature journal content. We may also use these personal data internally within ResearchGate and Springer Nature and as agreed share it, in an anonymised way, for purposes of tracking, analysis and reporting. We will not otherwise disclose your personal data outside the ResearchGate or the Springer Nature group of companies unless we have your permission as detailed in the Privacy Policy.

While Users may use the Springer Nature journal content for small scale, personal non-commercial use, it is important to note that Users may not:

1. use such content for the purpose of providing other users with access on a regular or large scale basis or as a means to circumvent access control;
2. use such content where to do so would be considered a criminal or statutory offence in any jurisdiction, or gives rise to civil liability, or is otherwise unlawful;
3. falsely or misleadingly imply or suggest endorsement, approval, sponsorship, or association unless explicitly agreed to by Springer Nature in writing;
4. use bots or other automated methods to access the content or redirect messages
5. override any security feature or exclusionary protocol; or
6. share the content in order to create substitute for Springer Nature products or services or a systematic database of Springer Nature journal content.

In line with the restriction against commercial use, Springer Nature does not permit the creation of a product or service that creates revenue, royalties, rent or income from our content or its inclusion as part of a paid for service or for other commercial gain. Springer Nature journal content cannot be used for inter-library loans and librarians may not upload Springer Nature journal content on a large scale into their, or any other, institutional repository.

These terms of use are reviewed regularly and may be amended at any time. Springer Nature is not obligated to publish any information or content on this website and may remove it or features or functionality at our sole discretion, at any time with or without notice. Springer Nature may revoke this licence to you at any time and remove access to any copies of the Springer Nature journal content which have been saved.

To the fullest extent permitted by law, Springer Nature makes no warranties, representations or guarantees to Users, either express or implied with respect to the Springer nature journal content and all parties disclaim and waive any implied warranties or warranties imposed by law, including merchantability or fitness for any particular purpose.

Please note that these rights do not automatically extend to content, data or other material published by Springer Nature that may be licensed from third parties.

If you would like to use or distribute our Springer Nature journal content to a wider audience or on a regular basis or in any other manner not expressly permitted by these Terms, please contact Springer Nature at

[onlineservice@springernature.com](mailto:onlineservice@springernature.com)